academicJournals

Vol. 8(12), pp. 456-465, 25 March, 2013
DOI 10.5897/SRE12.593
ISSN 1992-2248 © 2013 Academic Journals
http://www.academicjournals.org/SRE

Scientific Research and Essays

Full Length Research Paper

Magnetic field effect on phase separation process in a liquid mixture

Kachain Dangudom

Department of Physics, Faculty of Science, Naresuan University, Phitsanulok, 65000, Thailand.

Accepted 21 November, 2012

In this work, the statistical properties of the frequency distribution curves and the autocorrelation functions of the scattered photons from a laser beam incident on a liquid mixture approaching its phase separation temperature under an applied magnetic field in a dynamic light scattering experiment were employed in the study of the physical behavior of the scattering centers within the samples and in the calculations of their associated diffusion coefficients, respectively. It was found that while approaching the phase separation temperature, cluster formation of molecules of the same species occurred within the mixtures. Increasing the magnetic field strength resulted in enhancement of the effect. Our sample liquid mixtures exhibited phase separation behaviour when an applied magnetic field is strong enough.

Key words: Dynamic light scattering, photon correlation, density fluctuations, critical point.

INTRODUCTION

The physics of phase separation at the critical point is still not so clearly understood. As the critical point is approached, observation becomes difficult due to its instability behavior and very sensitive to any small changes of all physics conditions such as pressure, temperature, gravitational, magnetic and electric fields. Under certain conditions in a liquid mixture, where a well-mixed liquid mixture starts to separate into two phases, the light scattered off such a sample, caused by local density fluctuations in the scattering volume in thermodynamic equilibrium will have three different contributions (Berne and Pecora, 1976); one unshifted frequency, the Rayleigh line, results from entropy fluctuations and two frequency-shifted Brillouin lines are caused by pressure fluctuations of the liquid sample. The central unshifted peak can be analyzed to obtain the thermal diffusivity *D* of a liquid. A classical spectrum analysis procedure can be used to analyze the width of the scattered laser beam to obtain the diffusion coefficient *D* or a digital correlator can be used to obtain the time autocorrelation function which is the Fourier transform of the spectrum. In the dynamic light scattering technique, the number of photons received at the photo-detector is continuously counted and binned into consecutive bins of a fixed sample time for a certain length of time of the measurement; both the scattered intensity and the time correlation function can be studied from the same set of measured data.

The critical points of a one-component gas-liquid coexistence are related to a binary mixture. Theoretical insight suggests that the long range critical fluctuations are remarkably insensitive to the details of the intermolecular potential (Chu, 1974). Most of the work investigating phase separation phenomena in the past hardly found any evidence to suggest how the phase separation process does actually start physically. At the critical point of the phase separation process, the system becomes very sensitive to an external force of any form

E-mail: kachaind@nu.ac.th.

such as the gravitational field (Stanley, 1971). Up to the best of our knowledge, there is no work on magnetic field dependent phase separation; it is therefore interesting to study a phase separation process of a liquid-mixture under an applied magnetic field.

This experiment presents the study of the statistical fluctuations of the light scattered from the liquid mixtures approaching their phase separation temperatures under five different applied magnetic fields ranging from 0 to 80 mT using a dynamic light scattering technique. Both classical intensity measurements and the autocorrelation function technique were used to obtain light scattering intensity and thermal diffusivity properties of five compositions of the methanol/cyclohexane liquid mixtures close to their phase separation temperatures. Both the temperature and applied magnetic field strength dependences of the scattered intensity and thermal diffusivity were studied. The cluster formation within the samples was detected as the samples were reaching their phase separation temperatures. Overall pictures of the phase separation process at different temperatures under five different applied magnetic field strengths for all seven composition mixtures led to certain conclusions for the effect of the applied magnetic field on the liquid mixture phase separation.

THEORY

Light scattering and photon correlation spectroscopy

When a beam of linearly polarized light passes through a dielectric medium, the incident electric field induces an oscillating dipole of the same frequency at each point along its path. Each oscillating dipole radiates energy in all directions. The amplitude of the radiation scattered by a system of particles is simply the sum of the fields scattered by the individual particles, where the radiation phase from each particle, which depends on its position, is taken into account. In the case of Brownian motion of particle systems (Richard et al., 2005), the resultant amplitude in the far field fluctuates in magnitude and phase as the particles diffuse (Harding et al., 1993; Lipson, 1969). The intensity of the scattered light is a function of the wavelength λ, the scattering angle θ, the particle size d, and the relative index of refraction μ of the particle and the medium is given by:

$$I_{sc} = I_{in} f(\theta, \lambda, d, \mu) \quad (1)$$

In digital photon counting, a light scattering intensity measurement can be treated as a continuous photon counting process of *n(T),* where *n(T)* is the number of photons received in a time interval *T*. For the case of probability density analysis of the photon counts *n(T)*, the probability density function *f(m,T)* for *m* counts in an interval *T* can be expressed as:

$$f(m,T) = Np(q,T) \quad (2)$$

Where, *N* is the total number of photon counting operations of sample time *T* and *p(m,T)* is the probability of counting *m* photons in a sample time. The probability distribution function for any *n* counts for such a system of *N* operations can be written as:

$$F(n,T) = N \sum_{q=0}^{n} p(q,T) \quad (3)$$

The probability distribution function for all values of *n*, in time interval *T*, may be regarded as the density distribution function, *F(T)*. The peak position of *F(T)* is the most probable number of photons received in the time interval *T.* The density distribution function *F(T)* of the photon counts *n(T)* reflects the statistical properties of the laser beam light scattered by the scatterers. By theory, scattering off a fixed scatterer will give a delta function *F(n,T)* of a certain value of *n(T)*, while the Gaussian form of *F(n,T)* will be obtained for a sample undergoing a random process (Crosignami and Porto, 1975; Cummins and Pike, 1973). Higher scattering intensity is obtained in light scattering experiments from macromolecular solutions of higher molecular weight polymers under the same conditions, and the peak position of *F(n,T)* is moved to higher values of *n(T)*. For the case of a change in size of the scatterers, the peak-position of the probability distribution function *F(T)* should move accordingly. In a light scattering study of a phase separation at the critical point, the change in light scattering intensity is caused by the local density fluctuation in the sample and it increases rapidly on approaching the critical point leading to the phenomenon known as critical opalescence. The peak position of *F(T)* can be studied as a guide to give a better understanding of the phase separation process within a liquid mixture.

In the dynamic light scattering measurement, the measured intensity I_{sc} is replaced by the number of photons arriving at the photo-detector in a time interval *T, n(T),* and they can be treated further to form a time correlation function $\Gamma(\tau)$ defined as:

$$\Gamma(\tau) = \sum_{0}^{\infty} n(t) n(t+\tau) \quad (4)$$

where *n(t)* and *n(t+τ)* are the photon counts in a fixed sample time *T* at time *t* and at a delayed time *t+τ* respectively. A correlation function $\Gamma(\tau)$ gives information on the dynamic properties of the scatterers while a probability distribution function *F(T)* of the photon counts *n(T)* reflects the properties of the scatterers.

In the theoretical treatment of photon correlation spectroscopy for light scattered with a scattering vector ***k***, the average intensity correlation function *n(T)* takes the form (Leipertz et al., 1992).

$$\Gamma(k,\tau) = \langle n(k,0) n(k,\tau) \rangle \quad (5)$$

while the normalized form $g^{(2)}(k,T)$ is

$$g^{(2)}(k,\tau) = \frac{\langle n(k,0)n(k,\tau)\rangle}{\langle n(k,0)\rangle^2} = 1 + \beta\left|g^{(1)}(k,\tau)\right|^2 \quad (6)$$

where τ denotes the delayed time, and $n(k,\tau)$ is the scattered intensity at scattering vector $\boldsymbol{k}$, and $|\boldsymbol{k}|$ equals $(4\pi\mu/\lambda)\sin(\theta/2)$ for light of wavelength λ scattered from a liquid of refractive index μ at the scattering angle θ. β is a system constant of the setup while $g^{(1)}(k,\tau)$ and $g^{(2)}(k,\tau)$ are the first and the second order normalized time correlation functions respectively. The $g^{(1)}(k,\tau)$ is found to be the Fourier transform of the power spectrum of the scattered beam, and the $g^{(1)}(k,\tau)$ can be related to be:

$$g^{(1)}(k,\tau) = e^{-\xi\tau} \quad (7)$$

for the simple exponential case, where ξ is the decay rate for the k^{th} Fourier mode of the concentration fluctuations corresponding to the scattering vector $\boldsymbol{k}$ defined as:

$$\xi = D|k|^2 \quad (8)$$

where D is the diffusion constant obtained from $g^{(2)}(k,\tau)$. With an additional species of scatterer, $g^{(1)}(k,\tau)$ in the Equation (7) becomes:

$$g^{(1)}(k,\tau) = ae^{-\xi_1\tau} + be^{-\xi_2\tau} \quad (9)$$

where a and b are constants that depend on the scattering amplitude of each species of scatterer, while ξ_1 and ξ_2 are their corresponding decay rates. The normalized intensity correlation function has the form:

$$g^{(2)}(k,\tau) = 1 + \beta\left|ae^{-\xi_1\tau} + be^{-\xi_2\tau}\right|^2 \quad (10)$$

The computer curve fitting routine to a multi-exponential form of the time correlation function decay curve gives the diffusion coefficients of both species of scatterers.

Dynamics of phase separation of liquid mixtures

It is a well known fact that a rise in free energy, the rigorous thermodynamic criterion for a change of the system, is the main drive for mixing process of a liquid mixture. The change in free energy of the system is usually controlled by temperature and pressure, but can also be influenced by outside agencies (Schroeder, 2000; Morse, 1969). In this work, we chose a magnetic field as an external agent. When a magnetic field is applied to a homogeneous non uniform diamagnetic liquid mixture of two different species, A and B, the free energy of the system may be considered as consisting of two parts, one thermodynamic part, ΔF_{th} , and an additional part due to the presence of the magnetic field, ΔF_B.

In the following discussion we will follow the same assumption as in the paper of Mauri and Vladimirova (1999), namely, that diffusion is important only at the very beginning of the separation process, in that it creates a non-uniform concentration field. The H-model developed by Hohenberg and Haperin (1977) was employed for our phase separating liquid mixture.

The thermodynamic part of the free energy of mixing may be found in the following way. Let ϕ_A and ϕ_B be the volume fraction of the two liquid species. If there are N_A molecules of liquid species A, each in a volume Ω_A and N_B molecules of species B, each occupying a volume Ω_B, then the thermodynamic part of the free energy of mixing may be written as (Debye, 1959)

$$\Delta F_{th} = kT(N_A \ln\phi_A + N_B \ln\phi_B) + \frac{\alpha}{2}\frac{N_A\Omega_A N_B\Omega_B}{N_A\Omega_A + N_B\Omega_B} \quad (11)$$

Where α is an interaction parameter which we need not pay any attention here, k-the Boltzman constant and T the absolute temperature.

The magnetic part of the free energy is equal to (Griffiths, 1999):

$$\Delta F_B = -\frac{1}{2}\int \frac{B^2(\vec{r})}{\mu(\vec{r})} d^3r \quad (12)$$

Where $B(\vec{r})$ is the local field at point $\vec{r}$ obeying the appropriate boundaries conditions and μ is the permeability of the mixture. Normally, for a liquid mixture of two different species A and B with permeabilities μ_A and μ_B, respectively, μ will be dependent on the volume fraction $\phi(\vec{r})$ of the components. For wider and more rigorous theoretical treatment, for ones who are really interested in, could be found in for example the book of Landau Lifshitz (Landau and Lifshitz, 1984).

MATERIALS AND METHODS

In this experiment, the light scattering technique together with the technique of photon correlation spectroscopy (PCS) were used to measure the scattered intensities and the diffusion constants in the liquid mixtures of methanol and cyclohexane of seven mixture compositions, 27, 28, 28.5, 29, 29.5, 30 and 31% of methanol, at temperatures close to their phase separation temperatures. The chemicals used were AR grade without further purification. A micro-pipette with the accuracy of ±0.01 ml and 0.2 μm pore-size Acrodisc filters were used to ensure the correct composition and to remove dust from the samples. The sample temperature was controlled for each measurement to better than ±0.02°C by the SRS ac-resistance bridge temperature control system, SIM921, capable of controlling a preset-temperature within a 10^{-3} degree accuracy. The measurements were started at a high temperature where the methanol and cyclohexane were thoroughly mixed. The sample temperatures were allowed to decrease slowly to cover the phase-separation temperature where the two liquids just separated into two layers.

The modified water-cooled Cenco Zeeman effect electromagnet was used to generate a magnetic field in this experiment. The

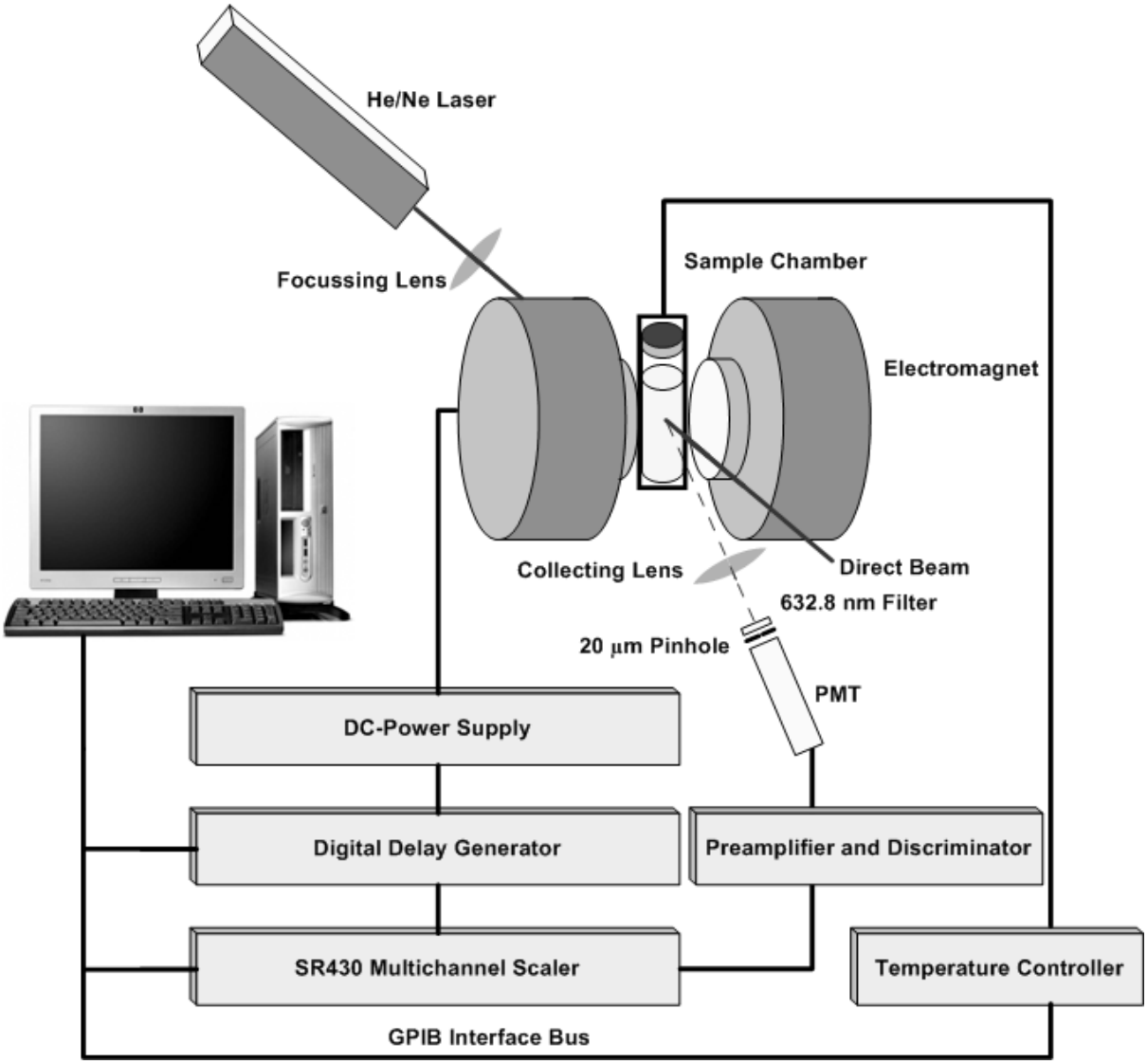

Figure 1. The schematic diagram of the experimental set-up.

electromagnet with 7.5 cm pole-diameter and 5 cm pole-gap was capable of generating a magnetic field of variable magnetic field strength from 0 to 90 mT by varying the dc coil current. The magnetic field strength was tested and calibrated using the Siemens KSY 14 ultra-flat Hall sensor. In the experiment, the temperature controlled chamber was placed centrally in the pole gap so that the center of the sample cell, which was the position of the scattering volume, was also located at the center to ensure a uniform magnetic field. The applied magnetic field strengths used in these experiments were 0, 20, 40, 60 and 80 mT.

The experimental setup was assembled on a vibration-free optical table, and a 35 mW He-Ne laser was used as a light source with vertical polarization perpendicular to the direction of the applied magnetic field. The beam was focused onto the center of the sample cell placed in the temperature controlled chamber. The forward scattering intensity was detected by a photomultiplier tube assembly at fixed scattering angle of about 6 degrees. The schematic diagram of the experimental setup is shown in Figure 1.

The photon-pulse train generated by the signal discriminator and amplifier circuits in the photo-detection assembly was fed directly to the photon counting system. The photon counts $n(T)$ of the sample time T were recorded continuously by the SR430 Stanford Research Systems multichannel scaler capable of counting fast pulse-trains up to 5 ns channel separation with a 32k memory bank. The 32k photon counts of each run were saved to a microcomputer memory. The measurement for each temperature was performed and recorded repeatedly for a 1000 runs to improve the signal-to-noise ratio of the experiment. The microcomputer was used both as a controller and a data acquisition device via the IEEE interface bus. The SRS digital delay generator DG535 was used for all timing and synchronization throughout the experiment. In the experiment, all the samples were studied under the same condition at 11 to 17 different temperatures under 5 different magnetic field strengths. In this work, a preliminary measurement was conducted and the acceptable sample time τ was found to be 81.92 μs. The untidy number 81.92 arises purely from the system clock timing logic of the SR430. The sample time 81.92 μs was used throughout the experiment. All the experimental control and data acquisition

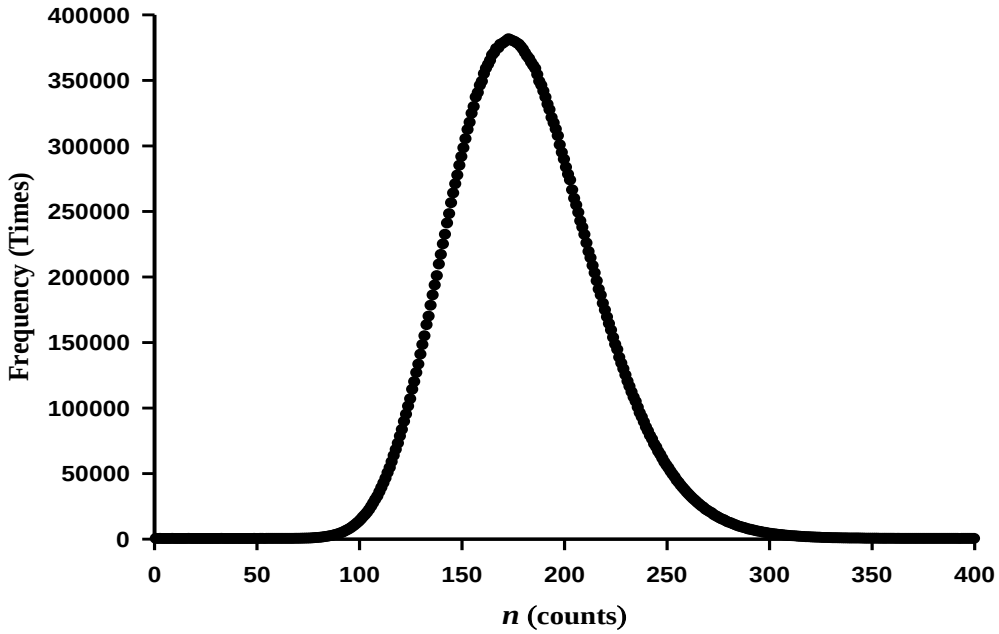

Figure 2. Frequency distribution curve for photon count *n(T)*.

routines, including sample temperature changes, were performed automatically under the software routines written in Turbo Pascal. The samples were kept about three hours at any desired temperature to ensure their thermodynamic equilibrium, and the temperature increments were around 10 to 100 mK depending on the closeness to the phase separation temperature.

All the recorded photon counts for each condition were used to form their associated frequency distribution curves for the scattered intensity study, while their time correlation functions were used to study the dynamic properties of the scattering centers. The frequency distribution curves and time correlation functions were then analyzed. The peak positions of the frequency distribution curves, the average photon count rate, were adopted as the relative scattered intensities for comparison among the conducted measurements. For the case of two peaks present in the frequency distribution curves, the double exponential form of $g^{(2)}(k,\tau)$ as indicated in Equation (10) was fitted to the time correlation function, otherwise the single exponential form was applied.

RESULTS

The light scattering measurements were performed on seven liquid mixtures at various compositions of methanol/cyclohexane from 27 to 31% of methanol by volume at temperatures ranging from 45.5 to 49°C in steps of approximately 0.1°C, under 5 different applied magnetic field strengths, and the following results were found.

Applied magnetic field intensity

The applied magnetic field was found to be very stable better than 0.5% across the central cross-sectional area of about 1 cm^2 while the scattering volume cross-section used in the experiment was about 80 µm diameter.

Frequency distribution curves

The frequency distribution curves for most of the experiments were in the Gaussian form as expected. The peak position shifted to higher values if the scattered beam was more intense. Typical frequency distribution curves of the photon counts at a point not too close to the phase separation temperature is shown in Figure 2, while Figure 3 is the curve obtained when the system temperature was very close to the phase separation temperature. These two curves serve as evidence to support the cluster formation process in the liquid mixture as found in this study.

Scattered intensity at various magnetic field strength

At any applied magnetic field strength, as the samples were cooled down slowly to their phase separation temperatures, the scattered intensity became stronger while the calculated diffusion coefficients decreased. The associated experimental results are shown in Tables 1 and 2 respectively.

Magnetic field effect on frequency distribution curves

For all samples under study, the applied magnetic field

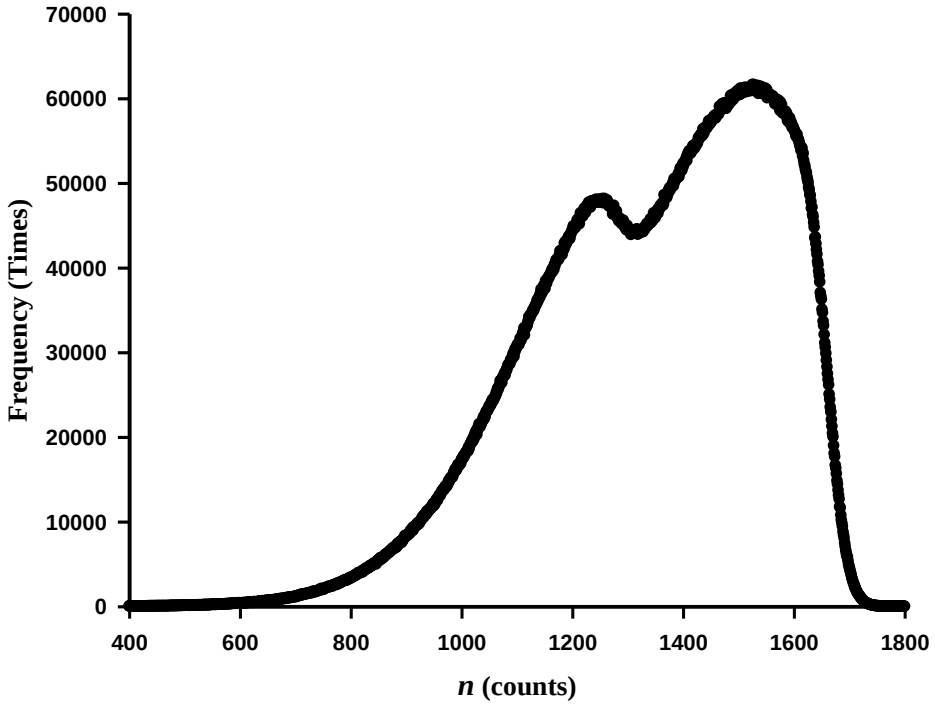

Figure 3. Frequency distribution curve for photon count *n(T)* for the case of more than one species scatterers.

Table 1. Most probable counted photon at difference temperature and magnetic field strength for the 28.5% methanol liquid-mixture.

Temperature (K)	Most probable counted photon at magnetic field strength (counts) (mT)				
	0	20	40	60	80
322.212	3	3	3	3	3
321.109	5	5	5	5	5
320.574	8	8	8	8	7
320.052	13	12	12	12	12
319.846	18	18	18	18	18
319.642	26	26	26	27	27
319.441	58	59	59	59	58
319.390	82	87	85	85	83
319.340	111	120	117	117	115
319.290	254	304	316	307	295
319.265	1,464	1,638	1,535	1,621	1,633
319.240	1,527	1,597	1,619	1,583	1,599
319.191	24	24	23	22	20
319.141	15	15	14	14	14

affected the phase separation process for both the scattered intensity curves and diffusion coefficient curves in similar ways. Typical frequency distribution curves of the scattered intensity as the difference between the sample temperature and the phase separation temperature, ΔT, decreased at different magnetic field strengths obtained from the experiment as shown in Figures 4, 5, and 6 for the case of 29% methanol mixtures.

DISCUSSION

In this experiment, a thousand 32k photon-count data

Table 2. Diffusion coefficient at difference temperature and magnetic field strength for the 28.5% methanol liquid-mixture. The asterisks indicate two peaks in frequency distribution curve.

Temperature (K)	Diffusion coefficient at magnetic field strength ($m^2 s^{-1}$)				
	0 mT	20 mT	40 mT	60 mT	80 mT
322.220	2.61E-10	2.46E-10	2.44E-10	2.47E-10	2.43E-10
321.109	1.84E-10	1.79E-10	1.81E-10	1.82E-10	1.81E-10
320.574	1.58E-10	1.55E-10	1.53E-10	1.52E-10	1.52E-10
320.052	1.19E-10	1.17E-10	1.18E-10	1.16E-10	1.14E-10
319.846	1.02E-10	9.97E-11	9.97E-11	9.77E-11	9.56E-11
319.642	8.02E-11	7.87E-11	7.80E-11	7.77E-11	7.81E-11
319.441	5.86E-11	5.50E-11	5.51E-11	5.46E-11	5.33E-11
319.390	5.00E-11	4.76E-11	4.78E-11	4.77E-11	4.85E-11
319.340	4.59E-11	4.30E-11	4.35E-11	4.35E-11	4.29E-11
319.290	3.75E-11	3.64E-11	3.63E-11	3.61E-11	3.48E-11
*319.265	8.52E-11	7.71E-11	1.03E-10	7.84E-11	9.27E-11
	8.88E-11	1.60E-10	1.14E-10	1.50E-10	1.14E-10
*319.240	1.83E-10	1.91E-10	1.76E-10	1.61E-10	1.43E-10
	1.92E-10	1.98E-10	1.84E-10	1.68E-10	1.36E-10
319.191	8.27E-11	8.00E-11	7.95E-11	8.36E-11	8.73E-11
319.141	1.01E-10	1.05E-10	9.99E-11	9.50E-11	9.29E-11

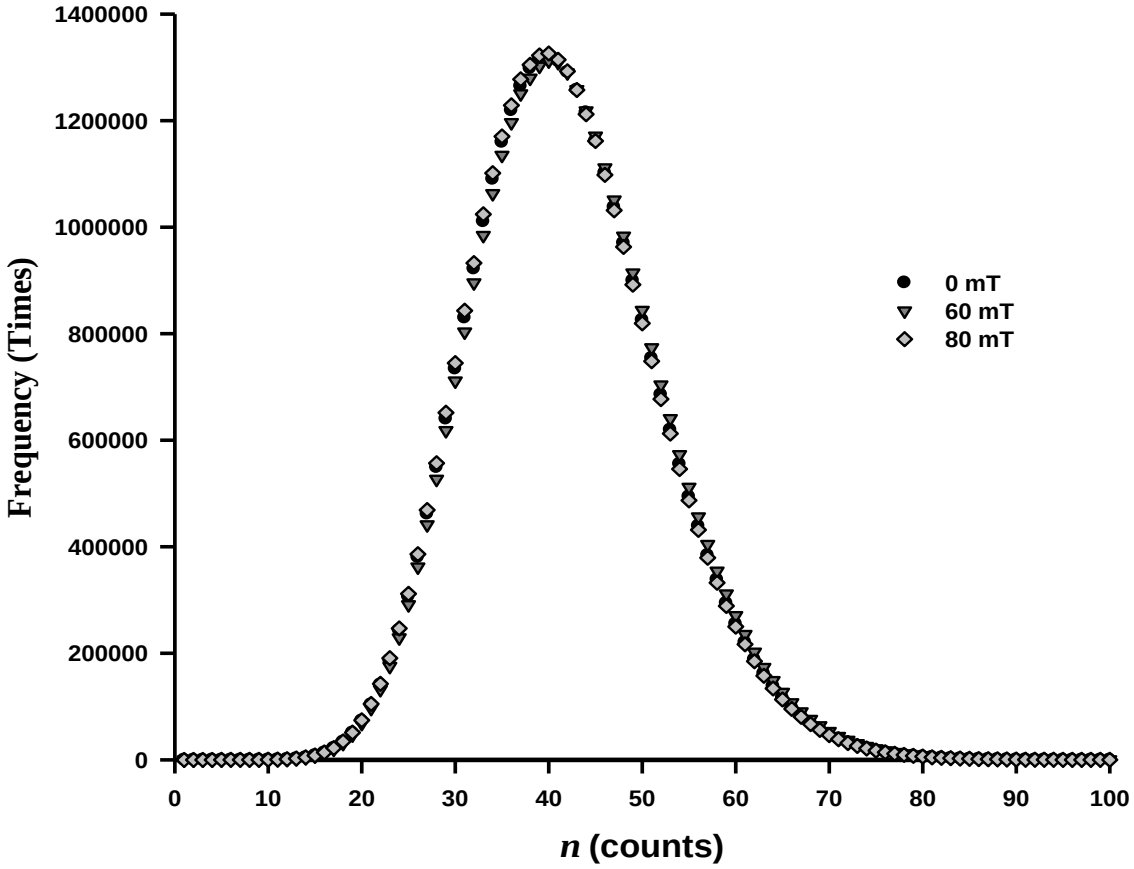

Figure 4. Frequency distribution curve for counted photons *n(T)* for three magnetic field strengths at temperature 319.642 K, ΔT = sample temperature - phase separation temperature = 277 mK, for the 29.0% methanol liquid-mixture.

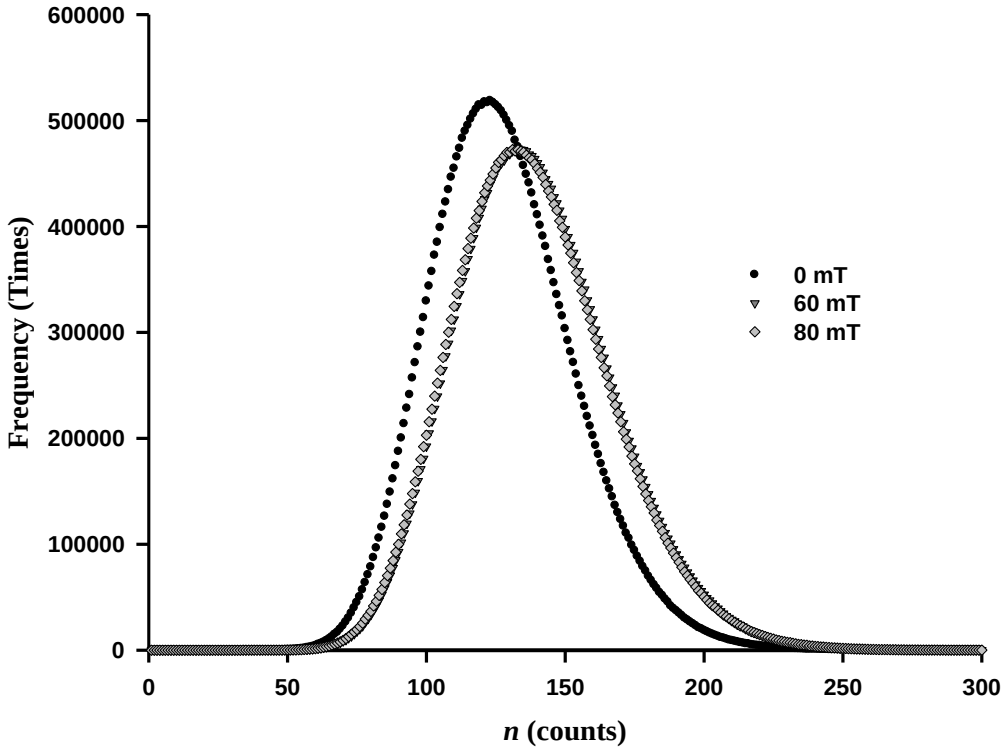

Figure 5. Frequency distribution curve for counted photons *n(T)* for three magnetic field strengths at temperature 319.441 K, ΔT = 76 mK, for the 29.0% methanol liquid-mixture.

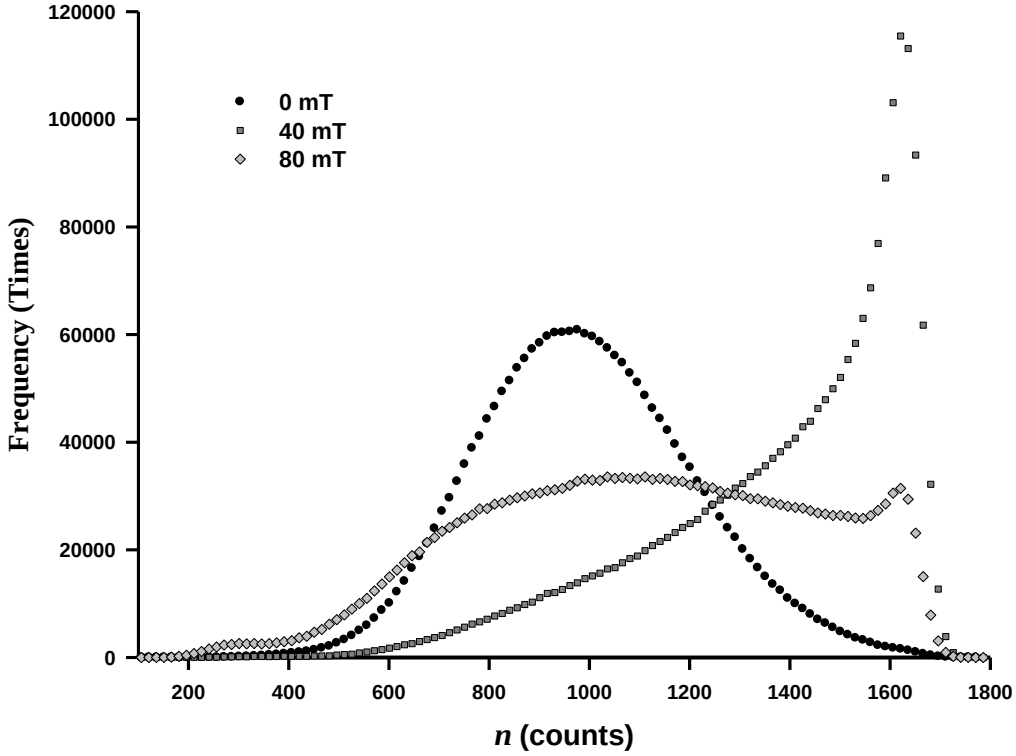

Figure 6. Frequency distribution curve for counted photons *n(T)* for three magnetic field strengths at temperature 319.375 K, ΔT = 10 mK, for the 29.0% methanol liquid-mixture.

were normally recorded in one measurement to ensurethe statistical accuracy of the measurements. It was found from the experiment that the statistical property of the photon-counts *n(T)* reflected the liquid-phase separation process in the mixtures. This process is supported by the existence of more than one species of the scattering centers within a mixture approaching its phase separation temperature as illustrated clearly for examples in Figures 2 and 3. It was also found from the experiment that when a magnetic field was applied to the system it had the effect of causing the phase separation process to occur earlier. In other words, increasing the applied magnetic field strength affected a liquid mixture in a similar manner to reducing the sample temperature. The results obtained can be summarized as follows.

Cluster formation in a liquid mixture

The Gaussian nature of the scattered intensity was distorted as the phase separation temperature was approached in all seven samples. This result arises from the fact that the scattering amplitudes from the scattering centers formed by both species were no longer random due to the differences in their molecular properties. This effect was more pronounced at higher applied magnetic field strength. The asymmetric nature of the photon-counts frequency distribution curve was further analyzed into detail as a cluster formation process in a liquid mixture on approaching the phase separation temperature of the same molecular species indicated by the multi-exponential form of the time-correlation functions, as indicated by the asterisk in Table 2. The associated diffusion coefficients of this scattering process were obtained from their time-correlation functions by fitting these data to the equation of the form $y = C_1+[C_2 \exp(-D_1K^2x) + C_3 \exp(-D_2K^2x)]^2$ for such the cases. From the values of D_1 and D_2 one could get their scattering size ratio using the assumption of a hard-sphere diffusion model with the equation $D=6\pi\eta a$ where D is the diffusion coefficient, η is the viscosity, and a is the hydrodynamic radius of the sphere. For the case of 29.5% methanol liquid mixture at 319.311 K under 60 mT applied magnetic field, the size-ratio of the scatterers was found to be 5.96 to 6.45 or 1 to 1.08 while the cyclohexane to methanol density ratio is 0.779 to 0.7918 which is 1 to 1.02. This indicates the phase separation process started to form a cluster of similar-nature molecular species, and can be detected by light scattering technique.

Magnetic field effect on phase separation

In most of the experimental, theoretical work will involve uniform and stationary state of the system under study. However, some works such as the study of electric field suddenly induced to the system (Tsori et al., 2004) or the introducing of charged particle into the system under study (Onuki, 2006) were also conducted. Those experiments introduced a transient effect into the system at the very unstable state as approaching the critical point of a mixture and introduced the system to more stable states. Some theoretical studies about the effect of fields on free energy of the system at the stationary state (Onuki and Kitamura, 2004; Moldover et al., 1979). This experiment is very difficult to find any significant evidences to illustrate the effect of magnetic field from scattered intensities and calculated diffusion coefficients at different magnetic field strength. However, for a sample at very close phase separation temperature, the effect of magnetic field strength on phase separation process is clearly observed from the frequency distribution curves as shown in Figures 4 to 6 for two composition mixtures. The effect might not appear very clearly in all results obtained in this experiment, to show how the drift of the peaks developed since the phase separation process is very sensitive to changes in all the parameters, and it is very difficult to approach an individual stationary condition as mentioned earlier. However, this can still be recognized by the drift of the maximum scattered intensities toward higher photon count rate when the applied magnetic field strength was increased, and this was true for all seven samples and it was found that this phenomenon is more sensitive as thermodynamic property of a sample is closer to its critical conditions. This phenomenon was found to be more sensitive as a sample temperature is very close, tens mK, to its phase separation temperature. A similar result for the gravitational effect on the phase separation process was found in a study with a sample in microgravity (Itami and Masaki, 2005). However, in this work, measurements of the permeability at different concentrations have not been performed which makes it not possible to calculate for the critical volume fraction. Therefore, it cannot be definitely stated whether the theory and the experimental results agree. It would be interesting to pursue the topic further in the future.

ACKNOWLEDGEMENTS

The authors would like to thank research scholarship of Naresuan University for any supported. The authors would like to thank Laser and applied optics laboratory at Chiang Mai University for the experimental device.

REFERENCES

Berne B, Pecora R (1976). Dynamic Light Scattering. Wiley & Sons, New York, p. 369.
Chu B (1974). Laser Light Scattering. Academic Press, New York, p291.
Crosignami B, Porto PD (1975). Statistical Properties of Scattered Light. Academic Press, London, p. 110.
Cummins HZ, Pike ER (1973). Photon Correlation and Light Beating Spectroscopy. Plenum Press, New York, p. 41.

Debye P (1959). Angular dissymmetry of the critical opalescence in liquid mixtures. J. Chem. Phys. 31: 680-687.
Griffiths DJ (1999). Introduction to Electrodynamics. Prentice Hall Inc., 3rd ed.
Harding SE, Sattelle DB, Bloomfield VA (1993). Laser Light Scattering in Biochemistry. The Royal Society of Chemistry, p. 66.
Hohenberg PC, Halperin BI (1977). Theory of dynamic critical phenomena. Rev. Mod. Phys. 49:435-479.
Itami T, Masaki T (2005). The critical behaviour under microgravity of liquid alloys with mutual immiscibility. Meas. Sci. Technol. 16:345-353.
Landau LD, Lifshitz EM (1984). Electrodynamics of Continuous Media. Pergamon Press, New York.
Leipertz A, Kraft K, Simonsohn G (1992). Determination of the sound velocity of transparent fluids near the critical point using photon correlation spectroscopy. Fluid Phase Equil. 79:201-210.
Lipson SG, Lipson H (1969). Optical Physics. Cambridge University Press, London, p. 300.
Mauri R, Vladimirova N (1999). Phase Separation of Liquid Mixtures. http://flash.uchicago.edu, university of Chicago, January.
Moldover MR, Sengers JV, Gammon RW, Hocken RJ (1979). Gravity effects in fluids near the critical point. Rev. Mod.Phys. 51:79-99.
Morse PM (1969). Thermal Physics. W.A. Benjamin. Inc., 2nd ed.
Onuki A (2006). Ginzburg-Landau theory of solvation in polar fluids: Ion distribution around an interface. Phys. Rev. E. 73:021506.
Onuki A, Kitamura H (2004). Solvation effects in near-critical binary mixtures. J. Chem. Phys. 121:3143-3151.
Richard P, Feynman P, Leighton BR, Sands M (2005). Feynman Lectures on Physics. Addison-Wesley Publishing Company, p. 411.
Schroeder DV (2000). An Introduction to Thermal Physics. Addison Wesley Longman.
Stanley HE (1971). Introduction to Phase Transitions and Critical Phenomena. Oxford University Press, London, p. 7.
Tsori Y, Tournilhac F, Leibler L (2004). Demixing in simple fluids induced by electric field gradients. Nature 430:544-547.